PAPER

The interfacial structure of polymeric surfactant stabilised air-in-water foams†

Jamie Hurcom,[a] Alison Paul,[a] Richard K. Heenan,[b] Alun Davies,[a] Nicholas Woodman,[c] Ralf Schweins[d] and Peter C. Griffiths*[e]

Small-angle neutron scattering was used to probe the interfacial structure of nitrogen-in-water foams created using a series of tri-block polymeric surfactants of the poly(ethylene oxide)–poly(propylene oxide)–poly(ethylene oxide) ($EO_x–PO_y–EO_x$) range, from which the nature of the polymeric interface could be characterised. The data follow a pronounced Q^{-4} decay, along with a number of inflexions and weak but well-defined peaks. These characteristics were well-described by a model embodying paracrystalline stacks of adsorbed polymer layers, whose formation is induced by the presence of the air–water interface, adsorbed at the flat air–water (film lamellae) interface. A minimum of approximately five paracrystalline polymer layers of thickness of the order of 85–160 Å, interspersed with somewhat thicker (400 Å) films of continuous aqueous phase were found to best fit the data. The thickness of the layer (L) was shown to follow a relationship predicted by anchor block dominated polymer adsorption theories from non-selective solvents, $L \sim EO^1PO^{1/3}$. The insight gained from these studies should permit a more rational design of polymeric stabilisers for hydrophilic polyurethane foams.

Introduction

Foams are dispersions of gas in an aqueous continuous phase and are formed in the presence of surfactant. Solid polymeric foams such as polyurethanes (PU) find use in a variety of applications including biomedical materials, insulation and soft furnishings.[1] The chemistry of these foams is well-documented involving step-growth polymerisation of di-isocyanate and polyalcohol monomers.[2] The structure and performance of PU foams is highly dependent on the surfactant behaviour at the air–liquid interface with the polymer chemistry locking in an otherwise transient structure.

It has long been known that small molecule and polymeric surfactants can be used to produce a stable foam, and more recently, colloidal silica nanoparticles have also been shown to adsorb at the air–water interface stabilising these interfaces[3,4] Foam destruction occurs *via* a number of processes:[5] drainage due to gravity or surface tension gradients; Ostwald ripening or coarsening driven by the diffusion of gas across thin films from smaller to larger bubbles; and bubble coalescence leading to the thinning and eventual rupture of thin films. By adsorbing at the air–liquid interface, surfactants lower the surface tension providing a surface elasticity mechanism, the Gibbs–Marangoni effect, that opposes localised film thinning.[6] However the ability to form persistent or long-lived foams is not solely dependent on this effect. The adsorbed surfactant layer must also have the ability to resist these depletion processes which is highly dependent on the structure of the adsorbed layer.

In the manufacture of solid polymeric foam, the stability of the wet foam has important consequences for cell window opening and porosity of the final cured polymeric foam. Thus, understanding the structure of surfactant at the air–water interface should allow greater insight into the role of polymeric stabilisers in polymeric foam systems.

Many attempts have been made to relate the structural and interfacial properties of non-ionic surfactants to aqueous single thin film and foam behaviour.[7–16] Conclusions have generally been qualitative, largely due to the inherent complexity of such foam systems, and a lack of detailed understanding of the assembly of stabilisers at the air–water interface. Against this context, the current study was conceived.

Small-angle neutron scattering (SANS) has been used previously to probe the structure of stabilisers at foam interfaces. The most elegant studies were presented by Axelos and Boue and co-workers[17] where they studied a series of dry and wet foams formed from aqueous solutions of the anionic surfactant sodium dodecylsulphate (SDS) at concentrations above and

[a]School of Chemistry, Cardiff University, Main Building, Park Place, Cardiff CF10 3TB, UK

[b]Science and Technology Facilities Council, Rutherford Appleton Laboratory, Harwell Oxford, Didcot, OX11 0QX, UK

[c]Polymer Health Technology, Festival Drive, Ebbw Vale, NP23 8XE, UK

[d]Institut Laue Langevin, Grenoble, Cedex 9, France

[e]Faculty of Engineering and Science, University of Greenwich, Central Avenue, Chatham Maritime, Kent ME4 4TB, UK. E-mail: p.griffiths@gre.ac.uk

below the critical micelle concentration (CMC). Both X-ray and neutron scattering were deployed. Under steady-state foaming conditions, wet films yielded a characteristic scattering pattern comprising a pronounced Q^{-4} dependence, with a number of superimposed peaks or "bumps". Through comparison with the solution scattering, these authors defined the foam interface as comprising two fully extended dodecyl chains (18.6 Å) separated by a water film of ~260 Å, with some additional features in the scattering arising from the micellar structures present within the aqueous regions of the wet foam (film lamellae). For the dry foams, the number of peaks was fewer, associated with the loss of the surfactant-like scattering from the aqueous regions.

In this work, we explore the nitrogen/water foams formed from ABA triblock copolymers of the poly(ethylene oxide)–poly(propylene oxide)–poly(ethylene oxide) type (EO_x–PO_y–EO_x), known commercially as Pluronics. Of principle interest is the analysis of small-angle neutron scattering data to probe the interfacial structure of surfactant in the foam from which the definition of the relationship between the molecular structure of the stabiliser and its foaming characteristics (ESI†) has been inferred.

Experimental

Materials

A series of structurally analogous poly(ethylene oxide)–poly(propylene oxide)–poly(ethylene oxide) tri-block polymeric surfactants known commercially as Pluronics were used as received, as listed in Table 1.

Solutions were prepared by dissolving various concentrations of the block copolymer in deuterated water (99.9%, Sigma Aldrich).

Small-angle neutron scattering

Foam generation. In all experiments, the foam sample was contained in a purpose built Perspex column of height 25 cm into which a 2 cm wide groove has been removed, and covered with aluminium foil to act as the neutron transparent windows for beam access, Scheme 1. Approximately 50 cm³ of surfactant solution was added to the sample holder at the base of the column. The foam is generated by bubbling gas through the frit at A. The neutron beam impinges on the aluminium foil

Scheme 1 SANS sample environment for studying foams.

between B and C behind which the Perspex has been partially removed. For stable foams, the reservoir D collects the foam sample and returns it to the base *via* the plastic tube at E. The heating jackets at F and G have been removed in this picture.

Steady state wet foams were studied in which a continuous air flow produces constantly regenerated foam. As such, the bubbles appear spherical and are separated by thick lamella walls. Experiments were conducted at room temperature. Experimental measuring times were approximately 5 minutes.

Instrument configuration. Small-angle neutron scattering experiments were performed on either (i) the time-of flight LOQ or SANS2d diffractometers at the ISIS pulsed Spallation Neutron Source, Rutherford Appleton Laboratory, Didcot, UK. Typically, a range defined by $Q = (4\pi/\lambda)\sin(\theta/2)$ between 0.005 and ≥0.3 Å⁻¹ is obtained by using neutron wavelengths (λ) spanning 2.2 to 10 Å (LOQ) or 1.75 to 16.5 Å (SANS2d) with a fixed sample–detector distance of ~4 m, or (ii) the steady-state reactor source, D11 diffractometer at the ILL, Grenoble where a Q range between 0.005 and 0.5 Å⁻¹ was obtained by choosing three instrument settings at a constant neutron wavelength (λ) of 8 Å and sample–detector distances of 1.2, 8 and 39 m.

All scattering data were (a) normalized for the sample transmission, (b) background corrected using the empty foam cell, and (c) corrected for the linearity and efficiency of the detector response using the instrument specific software package and the scattering from a polystyrene standard taped to the front of the foam cell.

Results and discussion

Small-angle neutron scattering was used to characterise the distribution of the polymer within the foam system whether that be dissolved in the aqueous regions or adsorbed at the interface. Accordingly, there may be several contributions to the measured scattering;

(1) any structure normal to the air–water interfaces, which would follow an approximate Q^{-4} dependence given that these interfaces would not be perfectly flat,

Table 1 Molecular weight and approximate composition characteristics of the Pluronic copolymers used in this work. The stated PEO composition is for both blocks

| Name | PPO block | | PEO block | | | Total MW/ | HLB |
	g mol⁻¹	Segments	g mol⁻¹	Segments	%	g mol⁻¹	
L62	1750	30	500	12	20	2500	1–7
PE6400	1750	30	1160	26	40	2900	7–12
P84	2250	43	1680	38	40	4200	12–18
P103	3250	60	1485	34	30	4950	7–12
P123	4000	70	1725	40	30	5750	12–18
P104	3250	60	2360	54	40	5900	12–18
PE6800	1750	30	6720	150	80	8400	>24
F108	3250	60	11 680	260	80	14 600	>24

(2) any in plane structure normal to the air–water interface,

(3) fluctuations in composition of the interfaces parallel to the beam,

(4) structures that would be present in the liquid junctions between bubbles, that may resemble "bulk solutions" at appropriate concentration, and,

(5) in aged, polyhedral foams, the long almost cylindrical regions at the junctions of bubbles associated with the plateau borders.

Representative data are presented in Fig. 1, and it is evident as suggested, that there are a number of features in the data. At low Q, the decay of the intensity with wavevector Q shows the pronounced Q^{-4} dependence, characteristic of the Porod scattering from a smooth interface of large radius. At high Q, there is a much slower decay, reminiscent of the solution scattering of these polymeric surfactants, into an incoherent background that varies for the four cases reflecting the fact that there is a different amount of sample in the beam in each case (the background is dominated by the incoherent scattering from the residual hydrogen content in the solvent as well as the polymer). Over the intermediate Q range, for three cases, there are noticeable points of inflexions, around $Q = 0.025$ and 0.04 Å^{-1}, associated with an oscillatory signature. For the P123 case, the scattering is far more intense, a point discussed in more detail later.

Focusing first on the high Q scattering, it is possible to identify this as the scattering from the polymeric surfactant in solutions comprising the plateau borders. Indeed, scattering from the appropriate solutions recorded in a conventional sample cell *e.g.* as in Fig. 2 (top), [PE6800] = 5% (w/v), can be overlaid onto the foam scattering, arbitrarily scaling the intensities after subtracting a flat incoherent background (a simplistic attempt to match the relative amounts of sample in the beam). Such an analysis was appropriate for the three cases, PE6400, PE6800 and L62, and to some extent P123. The high Q region of the data may therefore be associated with solution

Fig. 2 Small-angle neutron scattering from an air-in-water stabilised foam (circles) and a simple aqueous solution (squares) for polymeric surfactants PE6800 (top) and P123 (bottom). [Polymer] = 5% (w/v), arbitrarily scaled for comparison.

scattering, and indeed when fitted to the Debye model for a random coil polymer in solution, yielded radii of gyration typical of the appropriate molecular species *e.g.* R_g = 14 Å, 16.5 Å or 20 Å for PE6400, L62 and PE6800 respectively, in good agreement with dimensions obtained from an analysis of the solutions cell scattering for the monomeric species. Thus, it is concluded that for these systems there is a quantifiable contribution to the overall scattering from the polymer dissolved in the aqueous film forming the lamellae of the bubble.

The same conclusion may in fact be drawn from the P123 case, Fig. 2 (bottom), noting that the solution in this case is above its CMC and thus, the form of the scattering over both the intermediate and high Q regions is reminiscent of micellar rather than monomeric scattering, with an initial steeper decay at low Q.

Interestingly in this case, it is not possible to simultaneously overlay the (intensity of the) peaks associated with the inter-micellar structure factor ($Q = 0.03$ Å) and those associated with the core–shell morphology of the micelle ($Q = 0.1$ Å) implying that the structure of the micelle may be perturbed in the foam relative to the solution. Nonetheless, this initial data recorded on LOQ indicate that in order to isolate the foam scattering, the polymer concentration requires substantial dilution.

Fig. 3a and b present data recorded on D11 for two polymeric surfactants, over an extended Q range (compared to Fig. 1), as a function of dilution. The pronounced Q^{-4} is even more evident now due to the lower Q range accessed on this instrument
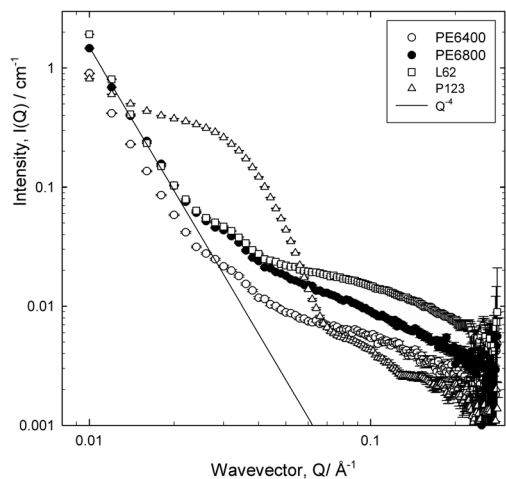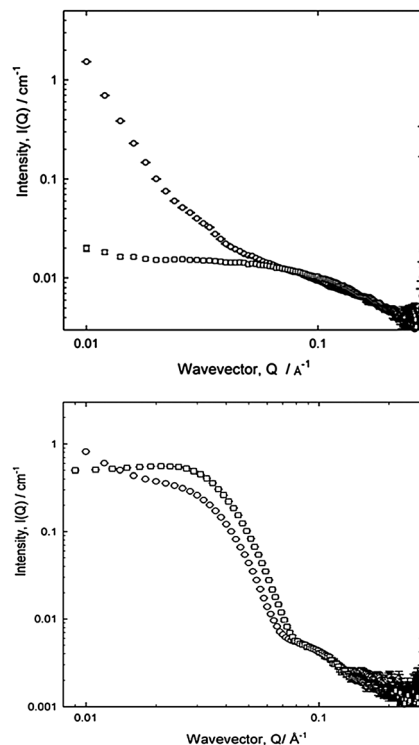

Fig. 1 Small-angle neutron scattering from foams stabilised by four polymeric surfactants with [Pluronic] = 5% (w/v). Gas flow varied slightly through this series in order to generate foam of sufficient height. Also shown is the low Q limiting value of Q^{-4}.
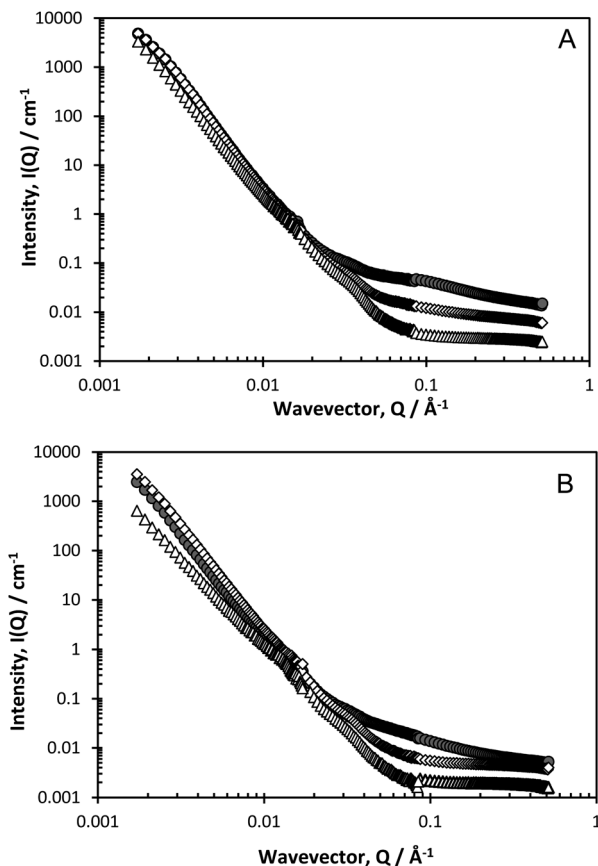
Fig. 3 (a) Small-angle neutron scattering for foams stabilised with polymeric surfactant PE6400 at various concentrations; 0.05% (w/v) (triangles), 0.5% (w/v) (diamonds) and 5% (w/v) (circles). (b) Small-angle neutron scattering for foams stabilised with polymeric surfactant F108 at various concentrations; 0.05% (w/v) (triangles), 0.5% (w/v) (diamonds) and 5% (w/v) (circles).
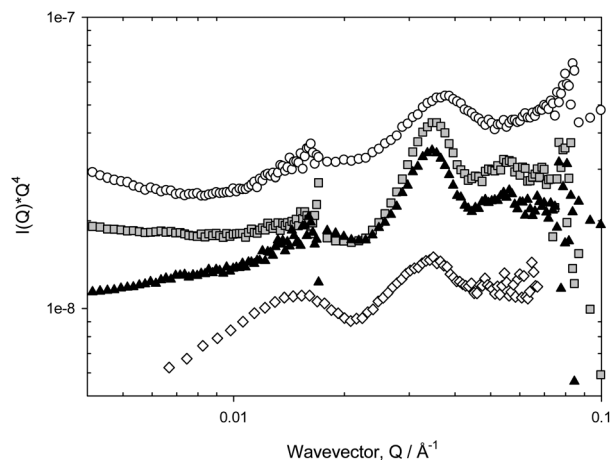

Fig. 4 Porod plot of small-angle neutron scattering from foams stabilised by four polymeric surfactants with [Pluronic] = 0.05% (w/v); PE6400 (circles), L62 (squares), PE6800 (triangles), F108 (diamonds).

(which could potentially introduce issues of multiple scattering), but the inflexion at $Q \approx 0.03$–0.04 Å^{-1} and the flat incoherent background at low polymer concentrations become more evident, as does a second inflexion at $Q \approx 0.01$–0.015 Å^{-1}.

The Porod region is valid when the size of the scattering object is larger than the range probed by the scattering radiation, and it is well-known that Q^{-4} behaviour characterises the smooth surfaces expected in foam systems. The points of inflexions in the scattering, as observed in Fig. 3a and b, can be highlighted by plotting the data on a Porod plot, $Q^4 I(Q)$ vs. Q, Fig. 4, as this effectively removes the Q^{-4} term. Well-defined peaks are now clearly evident at approximately $Q = 0.018$ Å^{-1} and $Q = 0.035$ Å^{-1}, though the positions of these peaks change slightly depending on surfactant type. The peak at $Q = 0.018$ Å^{-1} unfortunately overlapped with the edge of the detector used in one particular experimental geometry, but subsequent experiments confirmed this second peak to be real.

The observation of such correlation peaks of this nature clearly indicates the presence of regular structures, and since $r = 2\pi/Q_{peak}$, we may estimate $r = 180$ Å (± 10 Å) These cannot be attributed, as suggested by Axelos et al.,[17] to the total film thickness as the dimensions are inconsistent with this; bubble

lamella are estimated to be of micrometre size in the wet foams observed here. In addition, at 0.05% (w/v) the systems studied here are at concentrations significantly below their CMC, so the polymer concentration within the film lamellae are too dilute to contain micelles, thus we conclude also that the peaks cannot arise due to the presence (form factor) of aqueous micellar structures. Further, since the analysis of the solution scattering from these surfactants yields a radius of gyration of approximately 15–20 Å, in agreement with literature values,[18] it is also clear that this feature does not arise from molecular scattering. Therefore, we conclude that the foam introduces additional structure to the polymeric species near the interfaces.

Observations of such features in SANS data has previously been noted but not discussed; Zank et al.[19] reported lamellar Bragg peaks from high internal phase emulsions (HIPE) stabilised by Pluronic L92. Therefore, here, we have employed a model of the air–water interface that is assumed to consist of a para-crystalline stack of M thin polymer/water layers, of diffuseness T, thickness L and separation D,[20] to which is added if necessary, a Debye term to account for the solution scattering. The scattering length densities (contrast) of the various materials is such that in D$_2$O, the scattering arises equally from the air–D$_2$O and polymer–D$_2$O interfaces, and any further deconvolution of the data is not feasible (in this system at least). To limit the functionality of the fit, the diffuseness T has been constrained to $T = 0.01$. Typical starting values for the heterogeneity of L and D are $\sigma(L)/L$ and $\sigma(D)/D = 0.2$, though these values had little impact on the overall fit. Similarly, it was found empirically that a value of $M = 4$–6 was found to be the smallest necessary to produce suitable fits, and that larger values did not lead to appreciably better fits.

As may be seen from Fig. 5a and b, this model fits the experimental data rather well. The Q^{-4} term dominates the scattering so the accuracy of the parameters defining the inflexions are less than ideal, but the features are clearly reproduced in his approach. Pertinent parameters are given in Table 2. The heterogeneity in the surface structure varies with
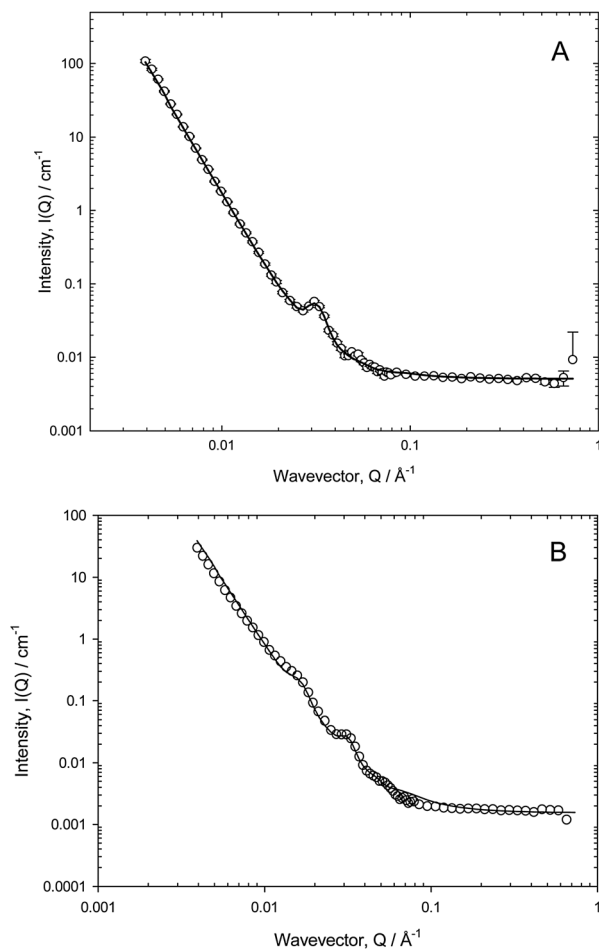
Fig. 5 (a) Small-angle neutron scattering from foams stabilised by 0.05% (w/v) L62 and the fit to the paracrystalline model described in the text. (b) Small-angle neutron scattering from foams stabilised by 0.05% (w/v) PE6800 and the fit to the paracrystalline model described in the text.

Table 2 Fit parameters to the scattering from Pluronic stabilised nitrogen-in-water foams (0.05% (w/v))

Name	L	$\sigma L/L$	M	D	$\sigma D/D$
PE6400	85	0.2	6	195	0.14
L62	90	0.22	6	195	0.15
P84	130	0.22	4	400	0.14
P103	150	0.27	4	400	0.15
PE6800	135	0.23	4	390	0.12
P104	145	0.24	3	400	0.13
P123	160	0.27	4	405	0.14
F108	220	0.25	4	430	0.14

surfactant in that PE6400 and L62 show only one peak in the scattering whereas P84, P103, PE6800, P104, F108 and P123 show two peaks.

In the various datasets, measured across the various instruments, the fitting routine is sensitive to which peak/inflexion is being fitted. For a perfectly crystalline stack, one would expect
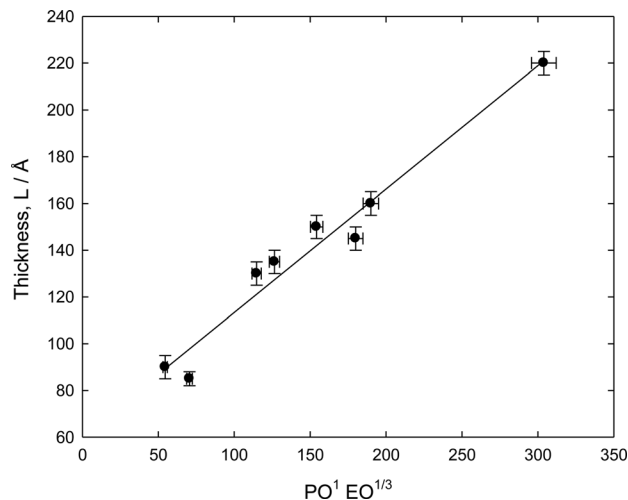

Fig. 6 Thickness of Pluronic [0.05% (w/v)] layers stabilising air-in-water foams, derived from the paracrystalline model described in the text recast in terms of a non-selective solvent polymer adsorption theory.

to see regularly spaced reflections at a common distance associated with $n = 1$, $n = 2$, $n = 3$ etc. Here, the separation D is slightly different whether the fitting routine focuses on the $n = 1$ ($Q = 0.015$ Å), or $n = 2$ ($Q = 0.035$ Å) peak. This implies that the structure is not a perfect lamellar one.

There is no obvious relationship between the thickness L and the molecular structure of the various Pluronic samples though L does seem to correlate more strongly with the PO content rather than the EO content, but also varies with the overall molecular weight. This behaviour is reminiscent of polymer adsorption from non-selective solvents.[21] Following a multi-variant analysis, a reasonable empirical correlation was found for the thickness data, $L \sim PO^1EO^{1/3}$, Fig. 6. This rather linear representation illustrates that the copolymer is forming a structure whose thickness is determined by the lateral association of the PO groups. The PO groups would therefore seem to be the dominating factor in terms of the structure, whereas the stability was found to correlate more strongly with the EO group characteristics, *viz.* PE6400 $\approx$ L62 < PE6800 < F108.

Conclusions

Small-angle neutron scattering has been deployed in an attempt to understand better the relative stabilities of air-in-water foams stabilised by a series of Pluronic block copolymers. A novel interfacial templated surfactant structure is observed, which may be interpreted as a paracrystalline stack of lamellae at the air–water interface. The thickness of these layers was shown to be dependent on both EO and PO block size characteristics, whereas the foam stability seems to correlate better with the EO block size, PE6400 $\approx$ L62 < PE6800 < F108, demonstrating a link between the nature of the adsorbed polymer layer and the overall composition and molecular weight of these poly(ethylene oxide)–poly(propylene oxide)–poly(ethylene oxide) (EO_x–PO_y–EO_x) copolymers.

Notes and references

1 D. Randall and S. Lee, *The Polyurethanes Book*, Wiley, New York, 2002.

2 C. S. Sipaut, N. Ahmad, R. Adnan, I. A. Rahman and M. N. M. Ibrahim, *Cell. Polym.*, 2010, **29**, 1–25.

3 A. Stocco, E. Rio, B. P. Binks and D. Langevin, *Soft Matter*, 2011, **7**, 1260–1267.

4 B. P. Binks and T. S. Horozov, *Angew. Chem., Int. Ed.*, 2005, **44**, 3722–3725.

5 D. K. Exerowa and P. M. Kruglyakov, *Foam and Foam Films; Theory, Experiment, Application* Elsevier, Amsterdam, NL, 1998.

6 R. J. Pugh, *Adv. Colloid Interface Sci.*, 1996, **64**, 67–142.

7 D. Exerowa and D. Platikanov, *Adv. Colloid Interface Sci.*, 2009, **147–148**, 74–87.

8 N. Kristen, A. Vullings, A. Laschewsky, R. Miller and R. von Klitzing, *Langmuir*, 2010, **26**, 9321–9327.

9 R. Petkova, S. Tcholakova and N. D. Denkov, *Langmuir*, 2012, **28**, 4996–5009.

10 E. Carey and C. Stubenrauch, *Colloids Surf., A*, 2013, **419**, 7–14.

11 R. Petkova, S. Tcholakova and N. D. Denkov, *Colloids Surf., A*, 2013, **438**, 174–185.

12 S. Samanta and P. Ghosh, *Chem. Eng. Res. Des.*, 2011, **89**, 2344–2355.

13 S. Samanta and P. Ghosh, *Ind. Eng. Chem. Res.*, 2011, **50**, 4484–4493.

14 T. Tamura, Y. Kaneko and M. Ohyama, *J. Colloid Interface Sci.*, 1995, **173**, 493–499.

15 T. Tamura, Y. Takeuchi and Y. Kaneko, *J. Colloid Interface Sci.*, 1998, **206**, 112–121.

16 Z.-L. Chen, Y.-L. Yan and X.-B. Huang, *Colloids Surf., A*, 2008, **331**, 239–244.

17 M. A. V. Axelos and F. Boue, *Langmuir*, 2003, **19**, 6598–6604.

18 K. Mortensen, *J. Phys.: Condens. Matter*, 1996, **8**, A103–A124.

19 J. Zank, P. A. Reynolds, A. J. Jackson, K. J. Baranyai, A. W. Perriman, J. G. Barker, M. H. Kim and J. W. White, *Phys. B*, 2006, **385**, 776–779.

20 M. Kotlarchyk and S. M. Ritzau, *J. Appl. Crystallogr.*, 1991, **24**, 753–758.

21 C. M. Marques and J. F. Joanny, *Macromolecules*, 1989, **22**, 1454.